Colloid and Polymer Science (2019) 297:1353–1363
https://doi.org/10.1007/s00396-019-04556-9

ORIGINAL CONTRIBUTION

# PSMA-*b*-PNIPAM copolymer micelles with both a hydrophobic segment and a hydrophilic terminal group: synthesis, micelle formation, and characterization

Xiaoyan Zhao [1,2] · Guorong Shan [1,2]

Received: 17 April 2019 / Revised: 16 August 2019 / Accepted: 19 August 2019 / Published online: 7 September 2019


## Abstract

Block copolymers of poly(*N*-isopropylacrylamide) (PNIPAM) with both a hydrophobic segment and a hydrophilic terminal group in the same chain were synthesized by reversible addition-fragmentation chain-transfer (RAFT) polymerization. One is a diblock copolymer with only hydrophobic poly (stearyl methacrylate) (PSMA) segment, while the other is a triblock copolymer with both a PSMA segment and a hydrophilic terminal group. Uniform spherical micelles were obtained. The triblock copolymer micelles showed a distinct evolution, first becoming small, then becoming larger, and finally becoming stable. The transition process was fast and reversible with temperature. Although the hydrophobic PSMA chain segment lowered the lower critical solution temperature of the diblock copolymer micelles, that of the triblock copolymer micelles was almost as high as that of the PNIPAM homopolymer. In the triblock copolymer, hydrophobic chains and hydrophilic segments co-existed, and their opposing effects partially canceled. The hydrophilic terminal group on the triblock copolymer made a great difference.

**Keywords** Poly(*N*-isopropylacrylamide) copolymers · Self-assembly · Hydrophilic terminal group · Thermo-responsive

## Introduction

Amphiphilic materials are widely encountered in nature and daily life. The most common examples are phospholipids in cell membranes and surfactants in detergents. They all consist of hydrophobic and hydrophilic segments and can self-organize into various morphologies [1–3]. They show excellent performances in different environments and attract wide research interest in many fields. Researchers are also trying to imitate these materials through chemical syntheses [4, 5]. Amphiphilic block copolymers are a typical class of synthetic amphiphilic materials. They can self-assemble into many different interesting morphologies in appropriate solvents, such as vesicles, spherical micelles, or cylindrical micelles. Moreover, the morphologies can be easily regulated and controlled by changing the chemical structures of the block species and the ratios between different blocks [6–10].

✉ Guorong Shan
shangr@zju.edu.cn

[1] State Key Laboratory of Chemical Engineering, College of Chemical and Biological Engineering, Zhejiang University, 38 Zheda Road, Hangzhou 310027, China

[2] Institute of Zhejiang University-Quzhou, Quzhou 324000, China

Smart polymers can be responsive to external stimuli such as pH, temperature, glucose, light, and so on. Combining both amphiphilicity and stimuli-responsiveness, materials can be simultaneously endowed with the two useful properties, offering wide applications in various fields, such as biology, drug loading [11], catalysis, and coating materials. Compared with other stimuli, temperature is more convenient to control and more easily applied. If one segment of a copolymer is thermo-responsive, its self-assembly behavior may be tuned by changing the temperature. Among the many thermosensitive materials, a typical example is poly(*N*-isopropylacrylamide) (PNIPAM). Scarpa et al. [12] first identified the thermo-sensitivity of PNIPAM in 1967. Because of hydrogen-bonding interactions between its amide groups and water, PNIPAM can undergo a reversible coil-globule transition process [13]. Diblock and triblock copolymers of hydrophilic monomers and NIPAM have been synthesized to systematically investigate their temperature-dependent micelle behavior. For example, Convertine et al. studied *N,N*-dimethylacrylamide (DMA) and NIPAM copolymers, which can form micelles at longer NIPAM chain lengths [6]. Poly (ethylene oxide) (PEO) is another common monomer used to form thermo-sensitive copolymers with NIPAM. It can assemble into vesicles in water and can be used to release drugs at 37 °C [7]. A linear amphiphilic

triblock copolymer of NIPAM and *tert*-Butyl acrylate (*t*BA) was synthesized and was found to adopt various morphologies, such as spherical micelles, cage-like micelles, and a layer structure [14]. Gradient copolymers of NIPAM can also be prepared to self-assemble into aggregates, which can respond rapidly to external stimuli [15]. Jellyfish-shaped amphiphilic dendrimers of poly (ethylene glycol) (PEG) and β-cyclodextrin (βCD) can also form extremely uniform aggregates in water [16]. Supramolecular multi-block copolymers can form particular morphologies with a high propensity for alternation [17]. Using random copolymers of *t*BA and DMA as a non-responsive core and PNIPAM as a corona, thermo-responsive behavior of the micelles can also be tuned by changing the core hydrophobicity [18].

Although a wide range of PNIPAM copolymers has been studied, block copolymers of PNIPAM with both hydrophobic and hydrophilic segments in the same chain are relatively rare. What is more, the different properties of diblock and triblock copolymer micelles were scarcely studied. In this work, two kinds of PNIPAM block copolymers have been synthesized by reversible addition-fragmentation transfer (RAFT) polymerization using two chain-transfer agents and then used to prepare micelles. One is a diblock copolymer comprising only hydrophobic segments, while the other is a triblock copolymer with both hydrophobic segments and a hydrophilic terminal group. Unexpected and interesting results have been obtained. A series of di- and triblock copolymers with constant hydrophobic block lengths and variable NIPAM block lengths has been synthesized to systematically study the interesting micelles. NMR and GPC have been applied to characterize the structures, and fluorescence measurements have been made to determine the critical micelle concentrations (CMCs). Micelle sizes were measured by dynamic light scattering (DLS), and lower critical solution concentrations were determined by UV/Vis spectrophotometry. TEM was used to characterize the microstructures of the micelles, and their microphase separation behavior was analyzed by small-angle X-ray scattering (SAXS).

## Experimental

### Materials

*N*-Isopropyl acrylamide (NIPAM, J&K Chemical) was purified by threefold recrystallization from *n*-hexane and dried in vacuo at 45 °C. The 2,2′-azobis (isobutyronitrile) (AIBN, Shanghai Shisihewei Chemical Co., Ltd.) was recrystallized from ethanol and dried in vacuo at 45 °C. The 1,4-dioxane was dried over molecular sieves. Stearyl methacrylate (SMA) and tetrabutylammonium hydrogen sulfate (THS) were purchased from J&K Chemical. Other reagents were purchased from Sinopharm Chemical Reagent Co. All reagents were analytical grade and were used as received unless specified otherwise. RAFT agents *S,S*′-bis(α,α'-dimethyl-α"-acetic acid)-trithiocarbonate (BDAAT) and 2-cyanopropan-2-yl dodecyl carbonotrithioate (CPDTTC) were synthesized according to previous literature reports [19–26]. Deionized water was used in the experiments.

### Synthesis of PSMA-*b*-PNIPAM copolymers

To control the structures of the copolymers, RAFT polymerization was adopted in this work. Using two different RAFT agents, two kinds of PSMA-*b*-PNIPAM copolymers with different structures were synthesized. The synthetic process involved two steps, as depicted in Scheme 1. A typical procedure was as follows.

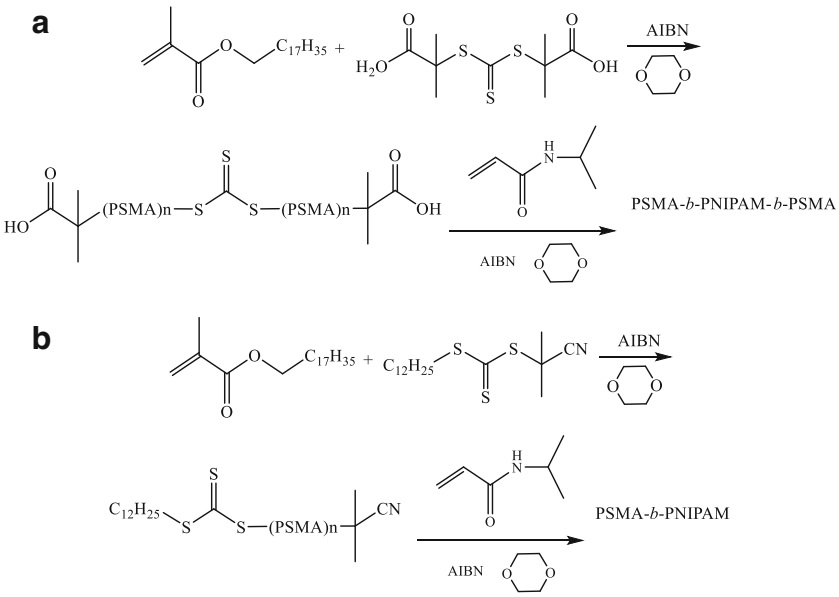


**Scheme 1** Synthesis process of **a** triblock and **b** diblock PSMA-*b*-PNIPAM copolymers

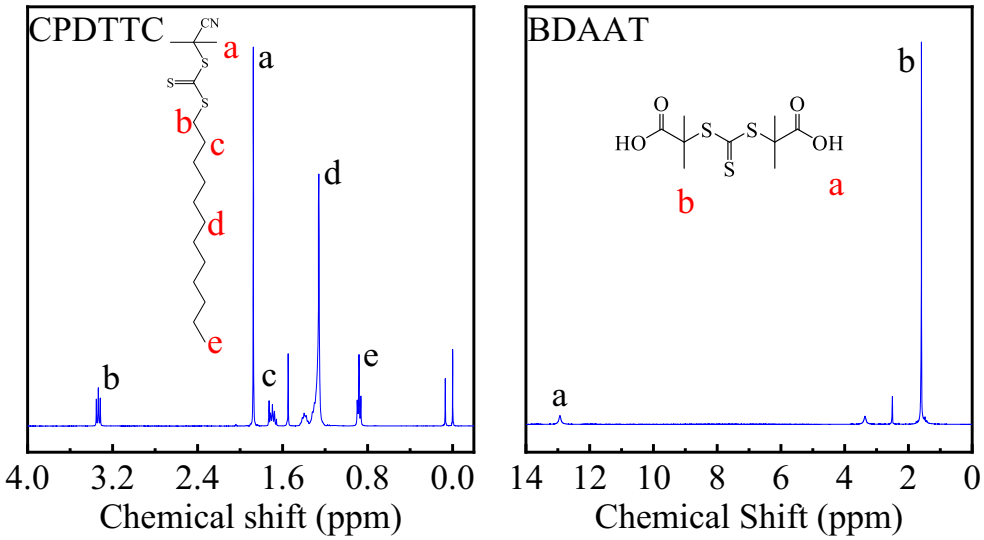


**Fig. 1** $^{1}$H NMR spectra of CPDTTC and BDAAT

Monomer SMA, RAFT agent, and 1,4-dioxane were mixed in a jacketed reactor. After bubbling with nitrogen for 30 min, the mixture was heated to 70 °C and AIBN was added to initiate polymerization. The first step was allowed to proceed for 6 h. The solution was then cooled to 10 °C, NIPAM monomer and 1,4-dioxane were added, and nitrogen was bubbled for 30 min. The mixture was heated to 70 °C once more, and further AIBN was added to initiate the reaction. The whole process was performed under nitrogen atmosphere. The final product was precipitated three times from *n*-hexane to remove unreacted monomers and 1,4-dioxane and then dried in vacuo. All reactions were carried out at a fixed SMA monomer mass (1 g) with various NIPAM monomer masses to obtain a series of PSMA-*b*-PNIPAM block copolymers. For diblock copolymers, CPDTTC (0.1699 g) was added; for triblock copolymers, BDAAT (0.1388 g) was added. The ratio of RAFT agent to AIBN was kept constant at 5:1.

## Preparation of micelles

The PSMA-*b*-PNIPAM copolymers were first dissolved in THF to obtain homogeneous solutions. To obtain micelles, the THF solutions were added dropwise to distilled water under magnetic stirring. The mixed solutions were then stirred for several days in open containers to allow the evaporation of THF. The aqueous solutions were at well above the CMCs of the copolymers and so could form stable micelles.

## Characterization

Chemical structures were characterized by recording $^{1}$H and $^{13}$C NMR spectra at ambient temperature on a 400-MHz Bruker AVANCE II NMR spectrometer (Bruker BioSpin Co., Switzerland). BDAAT was dissolved in deuterated dimethylsulfoxide ([$D_6$]DMSO), and other samples were dissolved in deuterated chloroform ($CDCl_3$).

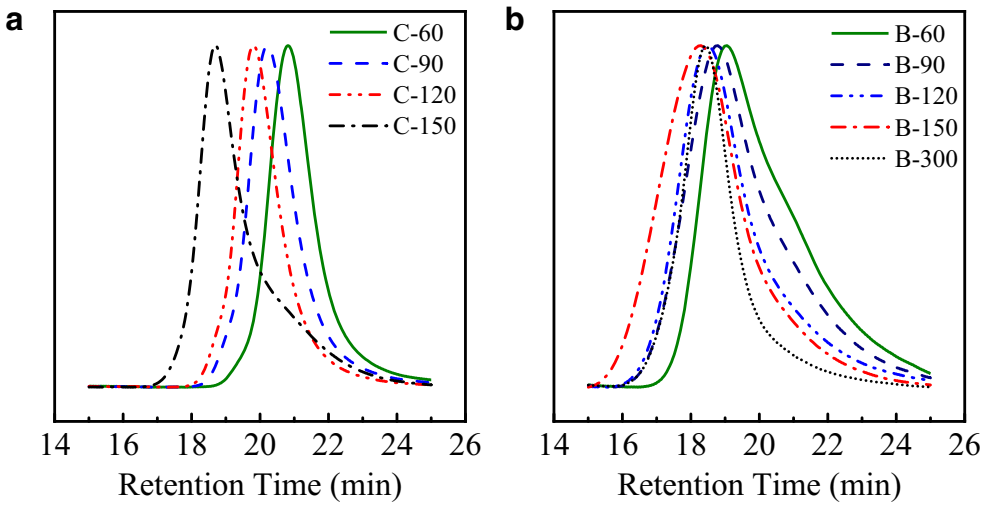


**Fig. 2** GPC traces of **a** diblock and **b** triblock PSMA-*b*-PNIPAM copolymers

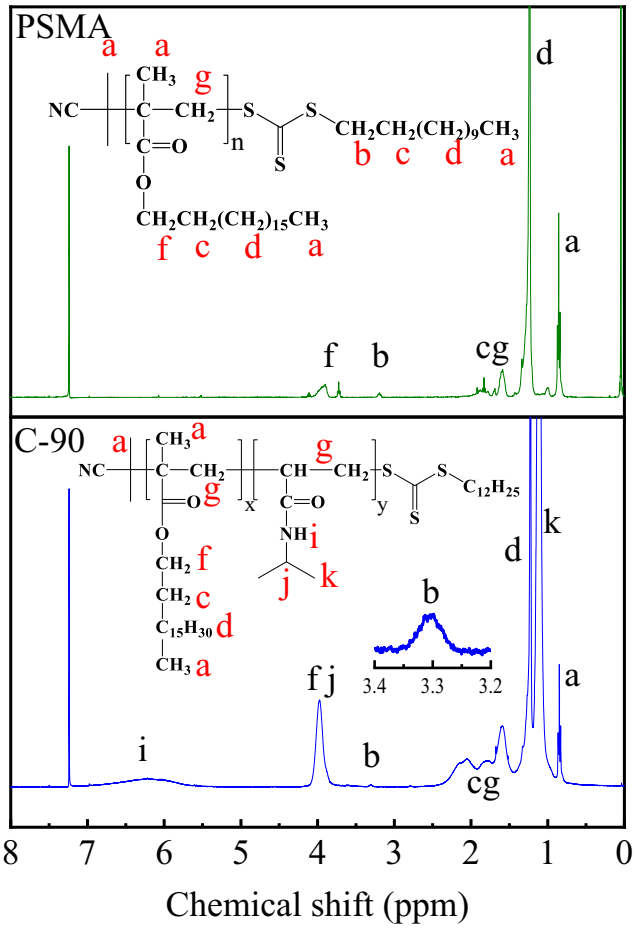


**Fig. 3** $^{1}$H NMR spectra of PSMA and PSMA-*b*-PNIPAM diblock copolymer (sample C-90) synthesized by CPDTTC

Molecular weights and molecular weight distributions were determined by gel permeation chromatography (GPC, Waters Co., Milford, MA, USA). DMF was used as eluent at a flow rate of 0.3 mL/min. Molecular weight was determined with reference to polystyrene standards. Micelle size was measured by dynamic light scattering (DLS) analysis on a Nano ZS 90 instrument (Malvern Instruments, Malvern, UK) with a 90° scattering angle. Each sample was measured three times from 10 to 60 °C at intervals of 5 °C. CMCs were determined by fluorescence measurements (Shimadzu RF-6000 Spectro) using pyrene as a polarity probe. Micelle solutions were prepared at various concentrations. An aliquot (4 μL) of a solution of pyrene in acetone (12.7 mg pyrene dissolved in 50 mL acetone) was placed in a volumetric flask (10 mL), the acetone was evaporated, and then the micelle solution was added. The measurement was carried out at an excitation wavelength of 390 nm, at a scanning speed of 600 nm/min. The lower critical solution temperature (LCST) was measured with a UV/Vis spectrophotometer (Shimadzu UV-1800) equipped with a temperature controller (Shimadzu S-1700). The temperature was raised from 10 to 70 °C at a rate of 1 °C min$^{-1}$. The absorbance at 500 nm was recorded, and the transmittance was calculated according to the Lambert-Beer law. The morphologies of the micelles were observed with a JEM-1230 transmission electron microscope (TEM, JEOL, Tokyo, Japan). Each micelle solution was dropped onto a carbon-coated copper grid, and water was removed with filter paper. Synchrotron radiation small-angle X-ray scattering (SAXS) analysis of the bulk copolymers was performed on the BL16B1 beamline of the Shanghai Synchrotron Radiation Facility (SSRF). The distance between the sample and the detector was 1800 mm, and the X-ray wavelength was 0.124 nm. 2D data were converted into intensities as a function of the scattering vector $\boldsymbol{q}$ ($\boldsymbol{q} = 4\pi\sin\theta/\lambda$), where $2\theta$ is the scattering angle [27–29].

## Results and discussion

Shorthand notations B and C were used to represent triblock and diblock copolymers, respectively, and numbers following the shorthand notations were the theoretical chain lengths of NIPAM.

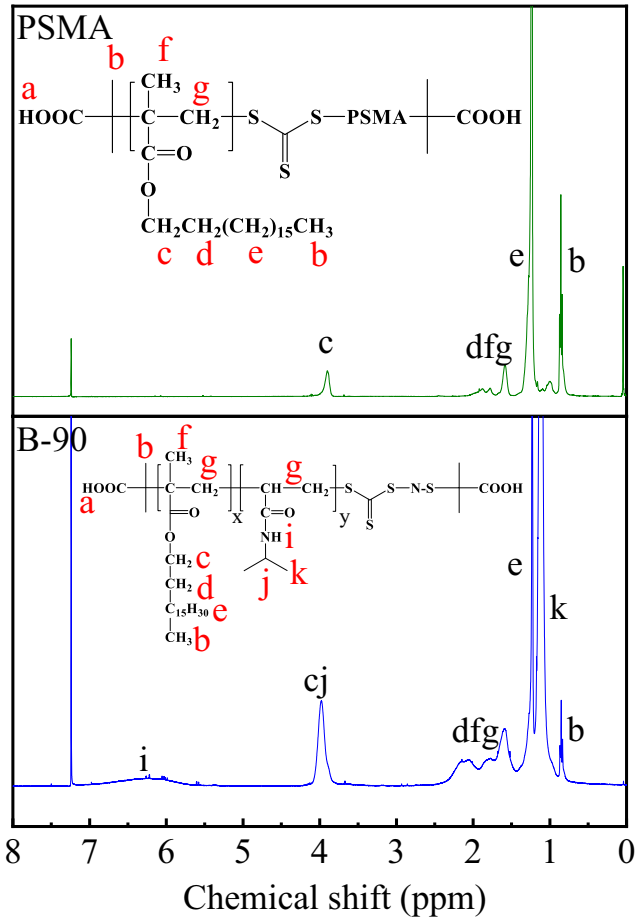


**Fig. 4** $^{1}$H NMR spectra of PSMA and PSMA-*b*-PNIPAM triblock copolymer (sample B-90) synthesized by BDAAT

## Structural characterization of the synthesized products

The chemical structures, compositions, and molecular weights of the synthesized RAFT agents and copolymers were determined by $^{1}$H, and $^{13}$C NMR and GPC measurements.

The key to success of RAFT polymerizations is the use of an appropriate chain-transfer agent (CTA). Given our desire to obtain both AB diblock and ABA triblock copolymers, two CTAs, namely CPDTTC and BDAAT, were synthesized according to literature procedures [19–26]. Figure 1 shows the assignment of each peak in their $^{1}$H NMR spectra. The peak area ratios are consistent with theoretical predictions, indicating that the target products were successfully obtained.

Two kinds of PSMA homopolymers at fixed molecular weights were used as macro chain transfer agents and narrowly distributed PSMA-*b*-PNIPAM copolymers were successfully synthesized. Figure 2 shows the GPC traces of the PSMA-*b*-PNIPAM copolymers. All of the traces are unimodal, indicating that the polymerization reactions were well controlled and there were no high molecular weight termination products.

Figure 3 shows the $^{1}$H NMR spectra of PSMA synthesized from CPDTTC and a PSMA-*b*-PNIPAM diblock copolymer (sample C-90), and Fig. 4 shows those of PSMA synthesized from BDAAT and a PSMA-*b*-PNIPAM triblock copolymer (sample B-90). Figure 5 shows the $^{1}$H NMR spectra of other diblock and triblock copolymer samples. The PSMA-*b*-PNIPAM copolymers were synthesized in two steps by RAFT polymerization. PSMA homopolymer was first synthesized, and then NIPAM monomer was added to form the second chain segment. The peak at $\delta \approx 3.90$ ppm can be assigned to methylene units adjacent to oxygen in SMA chains. The broad peak in the range 6–7 ppm can be attributed to –NH– in NIPAM chains. In Fig. 3, the small peak at $\delta = 3.15$ ppm can be assigned to methylene units adjacent to sulfur atoms in CPDTTC. The relative peak area ratios are almost consistent with the theoretical values. In the case of PSMA homopolymer and sample C-90 for example, the ratio of peak areas at $\delta = 3.15$ and 3.90 ppm for PSMA is about 1:6, as expected for the target homopolymer. For sample C-90, the ratio of peak area in the range $\delta = 6$–7 ppm to that at $\delta = 3.15$ ppm is about 50, near to the theoretical ratio (45).

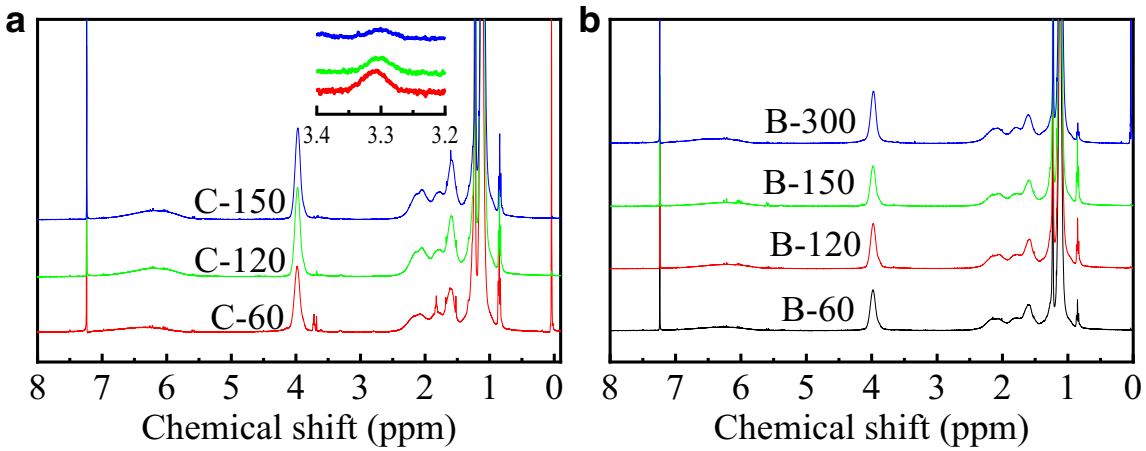


**Fig. 5** $^{1}$H NMR spectra of other **a** diblock and **b** triblock copolymer samples

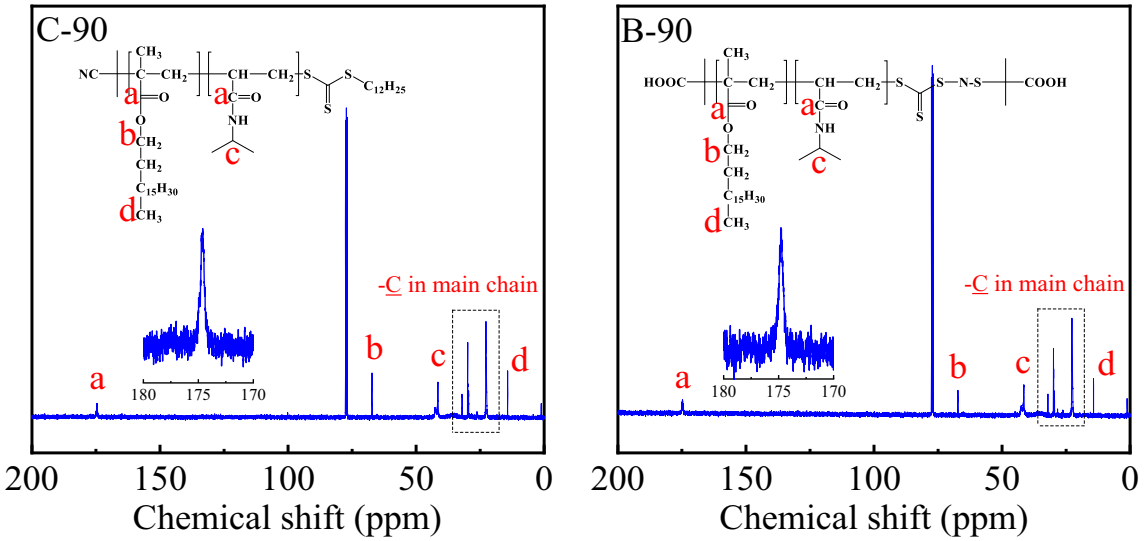


**Fig. 6** $^{13}C$ NMR spectra of PSMA-*b*-PNIPAM copolymers (sample C-90 and sample B-90)

To further confirm the structures of the copolymers, $^{13}C$ NMR spectra (samples C-90 and B-90) were measured, as shown in Fig. 6. The carbon signal of the methylene group adjacent to the oxygen atom appears at a fixed position (δ = 67 ppm), independent of components and substituent environments. Peaks at δ = 20–32 ppm can be assigned to carbon atoms in the main chain. According to previous literature reports [8, 30], peaks due to carbonyl carbon atoms were sensitive to structure differences, so they were selected to assess whether the products were block copolymers. If a sample is a random copolymer, the spectrum will show multiple peaks due to different sequences. Peaks at lower field can be ascribed to the SMA sequence and those at higher field to the NIPAM sequence. From Fig. 6, it can be seen that there was a peak at δ ≈ 174.5 ppm, attributable to a continuous NIPAM sequence. And there was an extremely weak peak at δ ≈ 177 ppm, attributable to a continuous SMA sequence, the peak was so weak that it mixed with the noise of baseline in $^{13}C$ NMR. In the copolymer chain, the theoretical ratio of the repeated units of SMA and NIPAM was 6:90, so compared to the NIPAM sequence, any continuous SMA sequence was too short, and its signal was too weak. Thus, we concluded that the final products were strict block copolymers.

## Micelle formation of the copolymers

Amphiphilic copolymers can self-assemble into different morphologies in appropriate solvents. In this work, spherical micelles of PSMA-*b*-PNIPAM block copolymers were formed by solvent evaporation from aqueous solution above their CMCs. CMCs were assessed by fluorescence measurements using pyrene as a polarity probe. The ratio of fluorescence excitation peak intensities at 339 and 333 nm is commonly used to express the polarity of the probe.[14] Pyrene was mixed with aqueous solutions of copolymers at different concentrations, and the intensities of the excited state were recorded. The ratio $I_{339}/I_{333}$ was plotted as a function of copolymer concentration. At low concentrations, this ratio maintained an almost constant value; but at higher concentrations, it increased linearly. The intersection point of the two slopes could be regarded as the critical concentration of the sample. As shown in Table 1, all of the copolymers displayed relatively low CMCs. For the same category of samples, the CMCs decreased with increasing chain length of NIPAM, albeit only slightly. All CMCs for the diblock copolymers were larger than those for the triblock copolymers, which might be attributed to hydrophilicity [31, 32]. When the samples are more hydrophilic, they can more easily form micelles. At low temperatures, a PNIPAM chain is hydrophilic. The terminal groups of CPDTTC, the CTA for diblock copolymers, cyano and methyl, are both hydrophobic. However, the terminal groups of BDAAT, the CTA for triblock copolymers, are hydrophilic carboxy. Hence, the obtained triblock copolymers were more hydrophilic than the diblock copolymers. In this work, the concentration used to prepare micelles was 0.1 mg/mL, well above the CMCs of the samples. Thus, it was expected that the copolymers would form micelles in aqueous solution.

**Table 1** Critical micelle concentrations of PSMA-*b*-PNIPAM copolymers (25 °C)

| Sample | CMC (mg/L) | Sample | CMC (mg/L) |
|---|---|---|---|
| C-60 | 15.85 | B-60 | 14.79 |
| C-90 | 14.13 | B-90 | 14.13 |
| C-120 | 13.80 | B-120 | 8.91 |
| C-150 | 9.33 | B-150 | 7.94 |
| | | B-300 | 8.66 |

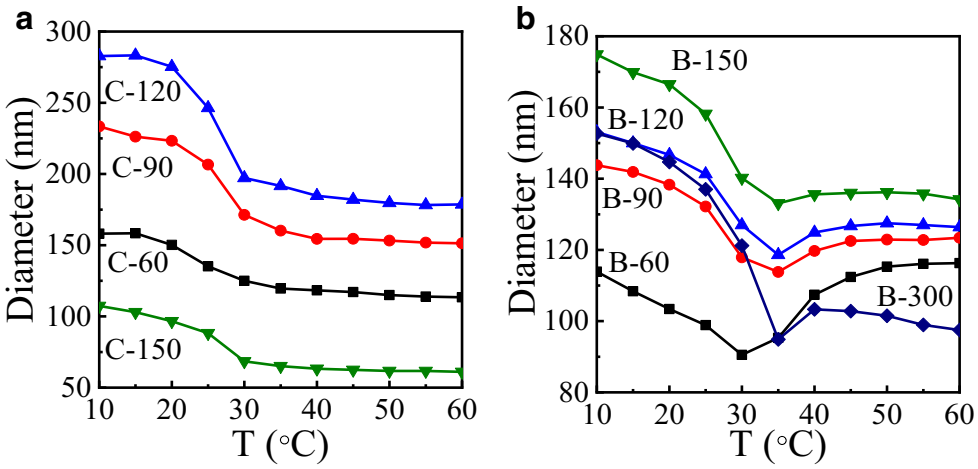


**Fig. 7** Change of micelle size with temperature measured by DLS. **a** Diblock. **b** Triblock

The sizes and morphologies of the copolymers were determined by DLS and using a TEM, respectively. Figure 7 shows the hydrodynamic diameters ($D_h$) of the micelles at various temperatures. It can be observed that the variations of micelle size were almost the same for the respective samples. With increasing temperature, the diameters of all samples decreased. The diameters of the micelles prepared from diblock copolymers became stable after an initial decrease, but, the diameters of those prepared from triblock copolymers subsequently increased slightly and finally became stable. These changes in the micelle size were reversible with temperature. The respective triblock and diblock copolymer micelles became larger with increasing NIPAM chain length. When the NIPAM chain length was shorter than a certain value, the sizes of micelles from the diblock copolymers were larger than those from the triblock copolymers.

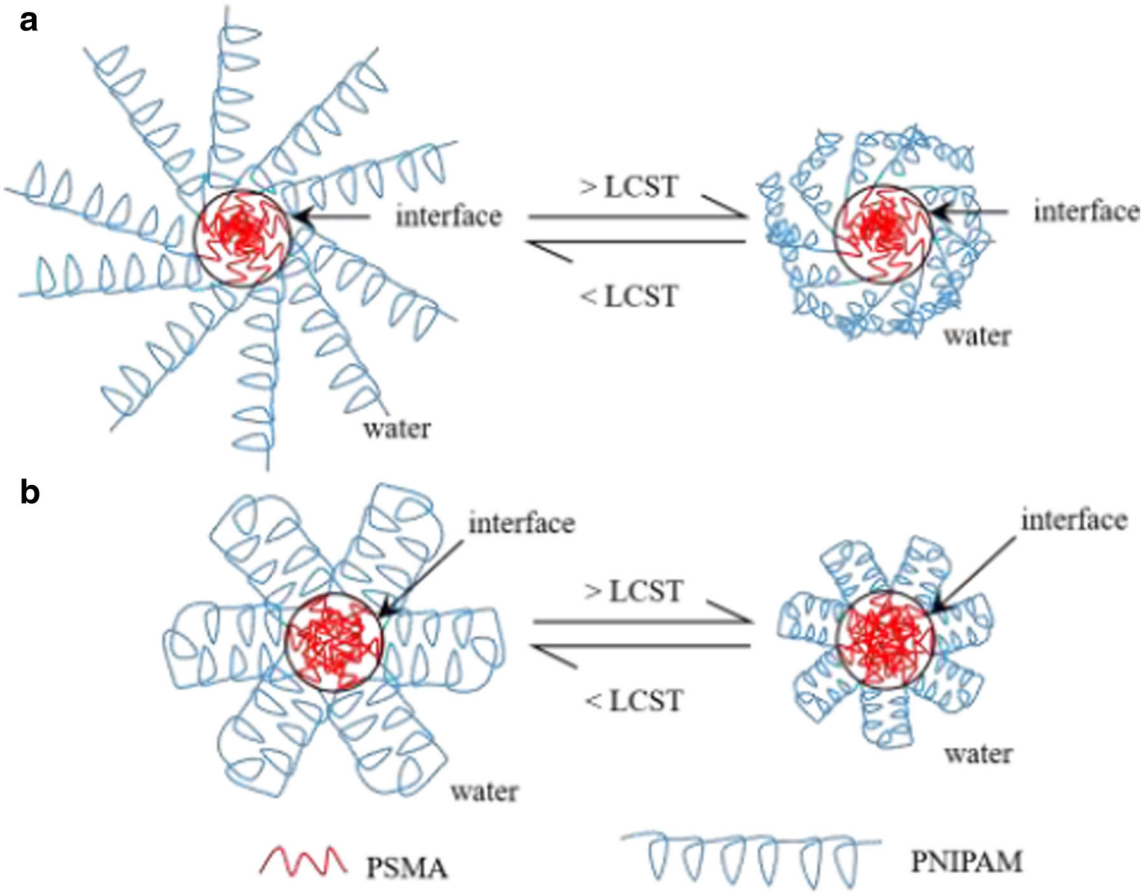


**Scheme 2** Schematic of PSMA-*b*-PNIPAM copolymer micelle transition with temperature. **a** Diblock. **b** Triblock

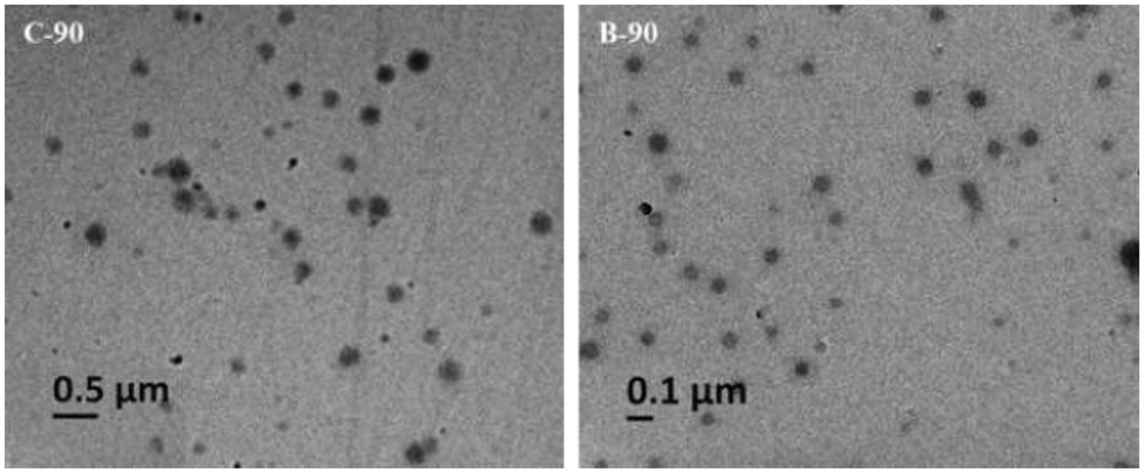


**Fig. 8** TEM image of micelles. **a** Sample C-90. **b** Sample B-90

According to the structures of the copolymers, the triblock copolymers were symmetrical and the PNIPAM chain was bisected by the thiocarbonylthio group when distributed in water, as depicted in Scheme 2. However, the PNIPAM chains in the diblock copolymers were fully extended. Therefore, when dispersed in aqueous solution, the micelle sizes of the diblock copolymers were much larger. This is also why the micelle sizes of samples C-60 and B-120 were similar. On increasing the temperature, the PNIPAM chain will shrink, so the micelle diameters will decrease. However, some micelles of the triblock copolymers will aggregate together, somewhat increasing the diameters. The shorter the NIPAM chain length, the more evident this change. When the NIPAM chain length is short, the proportion of the hydrophobic chain PSMA will be relatively large, facilitating aggregation. The specific process is depicted in Scheme 2. The DLS results are consistent with the TEM observations.

As shown in Fig. 8, uniform spherical particles were formed (samples C-90 and B-90 are shown as representative examples). When the NIPAM chain exceeded a certain length, the micelle sizes showed an abnormal tendency, as seen for samples C-150 and B-300. Their micelle sizes were smaller than those of the other samples. The longer the PNIPAM chain segment, the better the solubility of the copolymer, and its properties became more like those of PNIPAM homopolymer. The fact that the LCSTs of such co-polymers were close to that of pure PNIPAM reiterates this point. When the temperature is lower than the LCST of PNIPAM, the co-polymer can dissolve in water, but it cannot form micelles. The chain lengths of NIPAM in samples C-150 and B-300 were sufficiently long for their partial dissolution in water, but they could not completely dissolve like PNIPAM itself, so they could still form micelles. As a result, the sizes of the formed micelles were rather small.

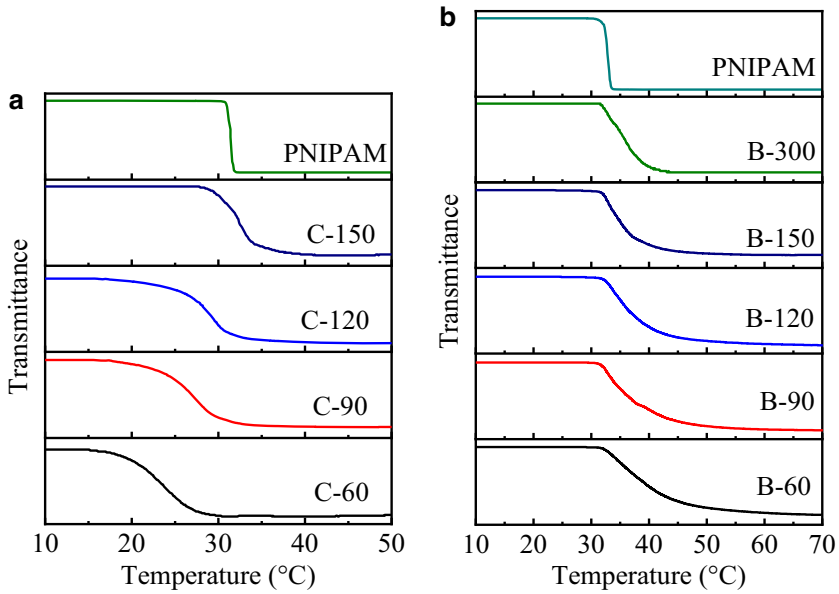


**Fig. 9** Temperature dependence of optical transmittance for **a** diblock and **b** triblock micelle solutions

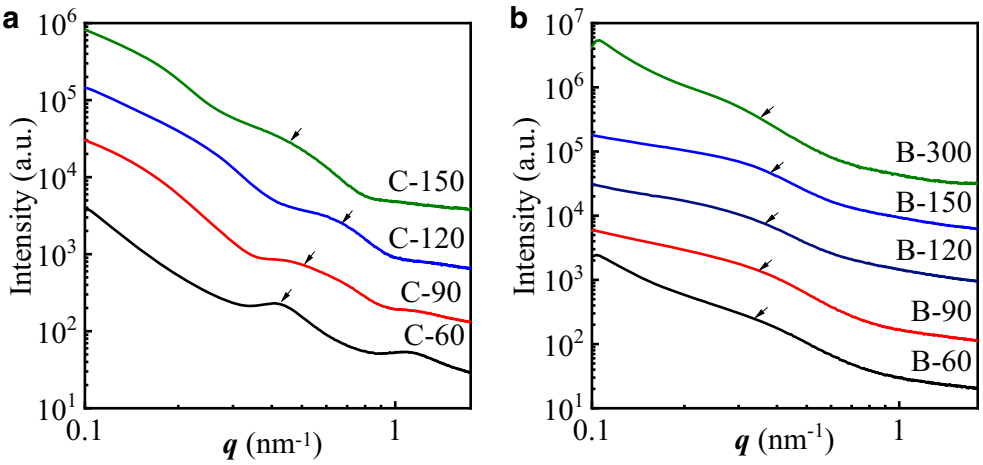


**Fig. 10** SAXS profiles of PSMA-*b*-PNIPAM **a** diblock and **b** triblock copolymers

In order to further study the thermo-sensitivity of the micelles, their LCSTs were measured by UV/Vis spectrophotometry. The results were consistent with the diameters measured by DLS. As shown in Fig. 9a, the LCSTs of diblock copolymer micelles were consistently lower than that of PNIPAM homopolymer, increasing with increasing of PNIPAM chain length. By copolymerization with hydrophobic monomers, the LCST was reduced. At a fixed chain length of PSMA, the longer the PNIPAM chain length, the higher the relative proportion of PNIPAM, and the closer the LCST to that of pure PNIPAM. The LCSTs of the triblock copolymer micelles were close to that of PNIPAM. The longer the PNIPAM chain length, the more quickly the transmittance becomes constant and the properties more closely resemble those of pure PNIPAM. There are both hydrophobic chains and hydrophilic terminal groups in the copolymers, and their opposing effects partially cancel. The hydrophilic group will increase the LCST [6, 7, 33–35], while the hydrophobic chain will lower it, as the net result of the two opposite effects, the LCSTs of the obtained micelles are unexpectedly close to that of PNIPAM.

To further investigate the formation mechanism of the micelles, synchrotron radiation SAXS analysis, a powerful tool for studying structural features of colloidal size [36, 37], was applied to analyze the bulk copolymers' microphase separation. For the amphiphilic copolymer systems, peaks in the SAXS patterns indicated the occurrence of microphase separation, and there was a regular arrangement between aggregations. As shown in Fig. 10, broad scattering peaks were seen for each sample, indicating weak microphase separation. The peaks became weaker with increasing NIPAM chain length, and samples C-60 and C-90 also showed another small peak at higher $q$. These phenomena revealed that when the PNIPAM chain length was shorter, the structure of the copolymers was better ordered, and the ordered structure of the crystalline side-chain PSMA was weakened by the amorphous PNIPAM chain. The average distance between aggregations can be calculated according to Bragg's law [38–40]:

$$d = \frac{2\pi}{q_{\max}} \tag{1}$$

where $q_{\max}$ is the $q$ value at the summit position of the related peak, and $d$ is the average distance between aggregations.

The calculated results are shown in Table 2. With increasing PNIPAM chain length, the average distance decreased, except for samples C-150 and B-300. The greater the distance between aggregations is, the smaller the micelle size will be. So the variation tendency of the distance between aggregations determined by SAXS was consistent with the variation tendency of the micelle sizes estimated by DLS. From the SAXS results, it can be seen that for both diblock and triblock copolymers, microphase separation occurred, leading to the formation of uniform spherical micelles.

**Table 2** Average distance between aggregations calculated by SAXS results

| Sample | $q$ ($nm^{-1}$) | $d$ (nm) | Sample | $q$ ($nm^{-1}$) | $d$ (nm) |
|---|---|---|---|---|---|
| C-60 | 0.43 | 14.61 | B-60 | 0.34 | 18.48 |
| C-90 | 0.51 | 12.32 | B-90 | 0.35 | 17.95 |
| C-120 | 0.68 | 9.24 | B-120 | 0.37 | 16.98 |
| C-150 | 0.46 | 13.66 | B-150 | 0.39 | 16.11 |
| | | | B-300 | 0.36 | 17.45 |

## Conclusions

Thermo-responsive micelles have been prepared based on hydrogen-bonding interactions between amide groups and water. The synthesized diblock and triblock copolymers could

self-assemble into uniform spherical micelles, and the micelle size varied reversibly with temperature. The size of the diblock copolymer micelles first decreased and then became stable. However, the size of the triblock copolymer micelles first decreased and then increased. This was because of some micellar aggregation. As the proportion of PSMA was increased, this phenomenon became more evident. The LCSTs of the diblock copolymers were all lower than that of PNIPAM homopolymer, consistent with previous literature reports. However, the LCSTs of the triblock copolymers were almost as high as that of PNIPAM homopolymer. The hydrophilic terminal group made a great difference. We have prepared novel thermo-sensitive micelles, the properties of which can be controlled by adjusting the chemical composition and the ratio of the different components. The materials showed great performances of all of their components and may find potential applications in controlled drug delivery or the loading and release of other nano-scale particles.

**Acknowledgments** We are grateful to BL16B1 beamline, Shanghai Synchrotron Radiation Facility, for SAXS measurements.

**Funding information** This work was financially supported by the National Natural Science Foundation of China (No. 21176210).

## Compliance with ethical standards

**Conflict of interest** The authors declare that they have no conflict of interest.

## References

1. Li XY, Gao Y, Boott CE, Winnik MA, Manners I (2015) Non-covalent synthesis of supermicelles with complex architectures using spatially confined hydrogen-bonding interactions. Nat Commun 6:8127
2. Li XY, Gao Y, Boott CE, Hayward DW, Harniman R, Whittell GR, Richardson RM, Winnik MA, Manners I (2016) "Cross" supermicelles via the hierarchical assembly of amphiphilic cylindrical triblock comicelles. J Am Chem Soc 138(12):4087–4095
3. Palmer LC, Stupp SI (2008) Molecular self-assembly into one-dimensional nanostructures. Acc Chem Res 41(12):1674–1684
4. Jeong B, Bae YH, Lee DS, Kim SW (1997) Biodegradable block copolymers as injectable drug-delivery systems. Nature 388(6645): 860–862
5. Pang XC, He YJ, Jung JH, Lin ZQ (2016) 1D nanocrystals with precisely controlled dimensions, compositions, and architectures. Science 353(6305):1268–1272
6. Convertine AJ, Lokitz BS, Vasileva Y, Myrick LJ, Scales CW, Lowe AB, McCormick CL (2006) Direct synthesis of thermally responsive DMA/NIPAM diblock and DMA/NIPAM/DMA triblock copolymers via aqueous, room temperature RAFT polymerization. Macromolecules 39(5):1724–1730
7. Qin SH, Geng Y, Discher DE, Yang S (2006) Temperature-controlled assembly and release from polymer vesicles of poly(ethylene oxide)-block-poly(*N*-isopropylacrylamide). Adv Mater 18(21):2905–2909
8. Xu XB, Shan GR, Pan PJ (2015) Amphiphilic quasi-block copolymers and their self-assembled nanoparticles via thermally induced interfacial absorption in miniemulsion polymerization. RSC Adv 5(62):50118–50125
9. Chang XH, Ma CL, Shan GR, Bao YZ, Pan PJ (2016) Poly(lactic acid)/poly(ethylene glycol) supramolecular diblock copolymers based on three-fold complementary hydrogen bonds: synthesis, micellization, and stimuli responsivity. Polymer 90:122–131
10. Chang XH, Bao JN, Shan GR, Bao YZ, Pan PJ (2017) Crystallization-driven formation of diversified assemblies for supramolecular poly(lactic acid)s in solution. Cryst Growth Des 17(5):2498–2506
11. Mao HL, Shan GR, Bao YZ, Wu ZL, Pan PJ (2016) Thermoresponsive physical hydrogels of poly(lactic acid)/poly(ethylene glycol) stereoblock copolymers tuned by stereostructure and hydrophobic block sequence. Soft Matter 12(20):4628–4637
12. Scarpa JS, Mueller DD, Klotz IM (1967) Slow hydrogen-deuterium exchange in a non-alpha-helical polyamide. J Am Chem Soc 89(24):6024–6030
13. Dimitrov I, Trzebicka B, Muller AHE, Dworak A, Tsvetanov CB (2007) Thermosensitive water-soluble copolymers with doubly responsive reversibly interacting entities. Prog Polym Sci 32(11): 1275–1343
14. Du BY, Mei AX, Yang Y, Zhang QF, Wang Q, Xu JT, Fan ZQ (2010) Synthesis and micelle behavior of (PNIPAm-P*t*BA-PNIPAm)$_m$ amphiphilic multiblock copolymer. Polymer 51(15): 3493–3502
15. Yañez-Macias R, Kulai I, Ulbrich J, Yildirim T, Sungur P, Hoeppener S, Guerrero-Santos R, Schubert US, Destarac M, Guerrero-Sanchez C, Harrisson S (2017) Thermosensitive spontaneous gradient copolymers with block- and gradient-like features. Polym Chem 8(34):5023–5032
16. Shao SQ, Si JX, Tang JB, Sui MH, Shen YQ (2014) Jellyfish-shaped amphiphilic dendrimers: synthesis and formation of extremely uniform aggregates. Macromolecules 47(3):916–921
17. Park T, Zimmerman SC (2006) A supramolecular multi-block copolymer with a high propensity for alternation. J Am Chem Soc 128(43):13986–13987
18. Blackman LD, Wright DB, Robin MP, Gibson MI, O'Reilly RK (2015) Effect of Micellization on the Thermoresponsive behavior of polymeric assemblies. ACS Macro Lett 4(11):1210–1214
19. Liang J, Shan GR, Pan PJ (2017) Aqueous RAFT polymerization of acrylamide: a convenient method for polyacrylamide with narrow molecular weight distribution. Chin J Polym Sci 35(1):123–129
20. Lai JT, Filla D, Shea R (2002) Functional polymers from novel carboxyl-terminated trithiocarbonates as highly efficient RAFT agents. Macromolecules 35(18):6754–6756
21. Chong YK, Krstina J, Le TPT, Moad G, Postma A, Rizzardo E, Thang SH (2003) Thiocarbonylthio compounds [SC(Ph)S−R] in free radical polymerization with reversible addition-fragmentation chain transfer (RAFT polymerization). Role of the free-radical leaving group (R). Macromolecules 36(7):2256–2272
22. Quinn JF, Rizzardo E, Davis TP (2001) Ambient temperature reversible addition–fragmentation chain transfer polymerisation. Chem Commun 11:1044–1045
23. Chiefari J, Mayadunne RTA, Moad CL, Moad G, Rizzardo E, Postma A, Skidmore MA, Thang SH (2003) Thiocarbonylthio compounds (SC(Z)S−R) in free radical polymerization with reversible addition-fragmentation chain transfer (RAFT polymerization). Effect of the activating group Z. Macromolecules 36(7):2273–2283
24. Mayadunne RTA, Rizzardo E, Chiefari J, Krstina J, Moad G, Postma A, Thang SH (2000) Living polymers by the use of trithiocarbonates as reversible addition-fragmentation chain transfer (RAFT) agents: ABA triblock copolymers by radical polymerization in two steps. Macromolecules 33(2):243–245

25. Moad G, Rizzardo E, Thang SH (2012) Living radical polymerization by the RAFT process—a third update. Aust J Chem 65(8):985–1076
26. Zhu Y, Bi SY, Gao X, Luo YW (2015) Comparison of RAFT Ab initio emulsion polymerization of methyl methacrylate and styrene mediated by oligo(methacrylic acid-*b*-methyl methacrylate) trithiocarbonate surfactant. Macromol React Eng 9(5):503–511
27. Liang J, Shan GR, Pan PJ (2017) Double network hydrogels with highly enhanced toughness based on a modified first network. Soft Matter 13(22):4148–4158
28. Takeno H, Obuchi K, Maki Y, Kondo S, Dobashi T (2011) A structural study of polyelectrolyte gels in a unidirectionally swollen state. Polymer 52(12):2685–2692
29. Wang LY, Shan GR, Pan PJ (2014) A strong and tough interpenetrating network hydrogel with ultrahigh compression resistance. Soft Matter 10(21):3850–3856
30. Aerdts AM, Eersels KLL, Groeninckx G (1996) Transamidation in melt-mixed aliphatic and aromatic polyamides .1. Determination of the degree of randomness and number-average block length by means of C-13 NMR. Macromolecules 29(3):1041–1045
31. Rub MA, Azum N, Khan F, Asiri AM (2017) Surface, micellar, and thermodynamic properties of antidepressant drug nortriptyline hydrochloride with TX-114 in aqueous/urea solutions. J Phys Org Chem 30(10):e3676
32. Zhang C, Luan HC, Wang GY (2018) A novel thermosensitive triblock copolymer from 100% renewably sourced poly(trimethylene ether) glycol. J Appl Polym Sci 135(14):46112
33. Xu XB, Shan GR, Pan PJ (2016) Controlled *co*-delivery of hydrophilic and hydrophobic drugs from thermosensitive and crystallizable copolymer nanoparticles. J Appl Polym Sci 133(42):44132
34. Kaneko Y, Yoshida R, Sakai K, Sakurai Y, Okano T (1995) Temperature-responsive shrinking kinetics of poly (*N*-isopropylacrylamide) copolymer gels with hydrophilic and hydrophobic comonomers. J Membr Sci 101(1–2):13–22
35. Lee WF, Hsu CH (1998) Thermoreversible hydrogels: 3. Synthesis and swelling behavior of the (*N*-isopropylacrylamide-*co*-trimethylacrylamidopropyl ammonium iodide) copolymeric hydrogels. Polymer 39(22):5393–5403
36. Lin YC, Wang YH, Zheng J, Yao K, Tan HY, Wang YT, Tang T, Xu DH (2015) Nanostructure and linear rheological response of comb-like copolymer PSVS-*g*-PE melts: influences of branching densities and branching chain length. Macromolecules 48(20):7640–7648
37. Noro A, Higuchi K, Sageshima Y, Matsushita Y (2012) Preparation and morphology of hybrids composed of a block copolymer and semiconductor nanoparticles via hydrogen bonding. Macromolecules 45(19):8013–8020
38. Geng YH, Lin XY, Pan PJ, Shan GR, Bao YZ, Song YH, Wu ZL, Zheng Q (2016) Hydrophobic association mediated physical hydrogels with high strength and healing ability. Polymer 100:60–68
39. Wang LY, Shan GR, Pan PJ (2014) Highly enhanced toughness of interpenetrating network hydrogel by incorporating poly(ethylene glycol) in first network. RSC Adv 4(108):63513–63519
40. Mable CJ, Thompson KL, Derry MJ, Mykhaylyk OO, Binks BP, Armes SP (2016) ABC triblock copolymer worms: synthesis, characterization, and evaluation as pickering emulsifiers for millimeter-sized droplets. Macromolecules 49(20):7897–7907